전력전자학술대회 논문집 1997. 7. 17-19 전력전자학회

적응 입출력 선형화 기법을 이용한 Brushless DC Motor의 강인한 속도 제어

김 경 화, 백 인 철, 문 건 우, 윤 명 중
한국과학기술원 전기및전자공학과

Robust Speed Control of Brushless DC Motor Using Adaptive Input-Output Linearization Technique

Kyeong-Hwa Kim, In-Cheol Baik, Gun-Woo Moon, and Myung-Joong Youn
Department of Electrical Engineering
Korea Advanced Institute of Science and Technology
373-1, Kusong-Dong, Yusong-Gu, Taejon, 305-701, Korea

Abstract **- A robust speed control scheme for a brushless DC (BLDC) motor using an adaptive input-output linearization technique is presented. By using this technique, the nonlinear motor model can be linearized in Brunovski canonical form, and the desired speed dynamics can be obtained based on the linearized model. This control technique, however, gives an undesirable output performance under the mismatch of the system parameters and load conditions. For the robust output response, the controller parameters will be estimated by a model reference adaptive technique where the disturbance torque and flux linkage are estimated. The adaptation laws are derived by the Popov's hyperstability theory and positivity concept. The proposed control scheme is implemented on a BLDC motor using the software of DSP TMS320C30 and the effectiveness is verified through the comparative experiments.**

I. INTRODUCTION

In most servo controller designs using BLDC motors, the electrical dynamics are often neglected because the electrical dynamics are inherently faster than the associated mechanical dynamics. By neglecting the electrical dynamics, the current is usually considered as a control input for the BLDC motor drive system having the high gain current feedback, and the speed controller is designed based on the first-order linearized model by a field-oriented control. This results in the cascaded control structure where the inner-loop current control and the outer-loop speed control schemes are separately designed [2]. Thus, it is more efficient to directly design the speed controller without using a separate inner-loop current regulator. Furthermore, robotics, machine tools, and direct drive motors are characterized as a smaller degree of dynamic time scale separation [3]. For these high performance drive applications, a conventional cascaded speed controller can not assure a high dynamic performance and a sufficient accuracy over the entire operating range. The effective approach to cope with this limitation is to directly design the speed controller considering the whole nonlinear motor dynamics.

In recent years, feedback linearization techniques have been applied to the control of the nonlinear plants such as the robot manipulators, induction motors, and BLDC motors [4]-[9]. The main objective is to force the speed [6], [7] and torque [8] of an induction motor or the speed of a BLDC motor [9] to follow their reference trajectories. By using these control strategies, the nonlinear terms can be effectively canceled out, and the output error dynamics can be specified based on the linear design techniques [4]. These techniques, however, require the full knowledge of the system parameters and load conditions. In general, BLDC motor drive systems are faced with unavoidable and unmeasurable disturbances or some parameter variations. Coupling the load to the motor shaft may cause the variations of the inertia and viscous friction coefficient besides the load variation. Also, the flux linkage varies nonlinearly with the temperature rise. In [9], an input-output linearization technique has been applied for the speed control of a BLDC motor. In this scheme, an integral control has been introduced to improve the robustness against the inaccurate speed measurement. However, other motor parameter variations have not been considered. Even though a steady-state response can be improved by introducing the integral control, it cannot give a good transient response under the parameter variations.

In view of the robustness against a load variation, it is well known that the use of a disturbance observer is very effective. Although the disturbance torque is not a state but an unknown inaccessible input, the conventional observer can be easily extended under the assumption that an unknown disturbance is a constant during each sampling interval [10], [11]. However, there is still a problem of parameter uncertainty since the flux linkage is not exactly known for a disturbance observer. An adaptive load torque observer against the variation of the flux linkage has been designed by the gradient method [11]. This method, however, generally requires two supplementary assumptions, i.e., the initial values of the estimated parameters must be in the neighborhood of the true parameters and the speed of the adaptation must be low [12].

In this paper, a robust speed control strategy of a BLDC motor using an adaptive input-output linearization technique is presented. Under the assumption that the disturbance torque and flux linkage are unknown parame-

ters, the input-output linearization is performed. The resultant model has the nonlinear disturbances in its input-output relation, which is caused by the unknown disturbance torque and the flux linkage variation. Applying the linear control law to such a model gives a steady-state output error as well as a deteriorated dynamic performance. To overcome these drawbacks, the disturbance torque and flux linkage will be estimated by using a model reference adaptive system (MRAS) technique and the adaptation laws are derived by the hyperstability theory and positivity concept. Since the nonlinear disturbances by the incomplete linearization can be effectively compensated by using this control scheme, a desired dynamic performance and a zero steady-state error can be obtained. The whole control processing is implemented by the software of DSP TMS320C30 for a BLDC motor driven by a three-phase voltage-fed PWM inverter.

II. MODELING OF BLDC MOTOR

The stator voltage equations of a BLDC motor in the synchronous reference frame are described as follows [1]:

$$v_{qs} = R_s i_{qs} + L_s \dot{i}_{qs} + L_s \omega_r i_{ds} + \lambda_m \omega_r \tag{1}$$

$$v_{ds} = R_s i_{ds} + L_s \dot{i}_{ds} - L_s \omega_r i_{qs} \tag{2}$$

where R_s is the stator resistance, L_s is the stator inductance, ω_r is the electrical rotor angular velocity, and λ_m is the flux linkage established by the permanent magnet. The speed dynamics is expressed as

$$\dot{\omega}_r = \frac{3}{2}\frac{p^2}{J}\lambda_m i_{qs} - \frac{B}{J}\omega_r - \frac{p}{J}T_L \tag{3}$$

where J is the moment of inertia of the rotor and its attached load, B is the viscous friction coefficient, p is the number of pole pairs, and T_L is the load torque. Using ω_r, i_{qs}, and i_{ds} as the state variables, the nonlinear state equation of a BLDC motor can be expressed as follows:

$$\dot{x} = f(x) + g_1 v_{qs} + g_2 v_{ds} \tag{4}$$

where $x = [\omega_r \quad i_{qs} \quad i_{ds}]^T$,

$$g_1 = \begin{pmatrix} 0 & \frac{1}{L_s} & 0 \end{pmatrix}^T, \quad g_2 = \begin{pmatrix} 0 & 0 & \frac{1}{L_s} \end{pmatrix}^T$$

$$f(x) = \begin{pmatrix} \frac{3}{2}\frac{p^2}{J}\lambda_m i_{qs} - \frac{B}{J}\omega_r - \frac{p}{J}T_L \\ -\frac{R_s}{L_s} i_{qs} - \omega_r i_{ds} - \frac{\lambda_m}{L_s}\omega_r \\ -\frac{R_s}{L_s} i_{ds} + \omega_r i_{qs} \end{pmatrix}.$$

III. INPUT-OUTPUT FEEDBACK LINEARIZATION

To linearize the nonlinear model in (4), the controlled variable is differentiated with respect to time until the input appears. This can be done by introducing the Lie derivative as follows [4]:

$$L_f h = \nabla h \cdot f = \sum_{i=1}^{n} \frac{\partial h}{\partial x_i} f_i(x) \tag{5}$$

$$L_f^i h = L_f(L_f^{(i-1)} h). \tag{6}$$

In order to avoid any zero dynamics, ω_r and i_{ds} are chosen as the outputs [9]. The objective of the control is to maintain the speed and d-axis current to their reference values or trajectories. For this objective, the new state variables are defined as follows:

$$y_1 = h_1(x) = \omega_r \tag{7}$$

$$y_2 = \dot{\omega}_r = L_f h_1(x) = \frac{3}{2}\frac{p^2}{J}\lambda_m i_{qs} - \frac{B}{J}\omega_r - \frac{p}{J}T_L \tag{8}$$

$$y_3 = h_2(x) = i_{ds} \tag{9}$$

where y_1 is the speed, y_2 is the acceleration, and y_3 is the d-axis current. The dynamic equations using the new state variables can be rewritten as follows:

$$\dot{y}_1 = y_2 \tag{10}$$

$$\dot{y}_2 = L_f^2 h_1 + L_{g1} L_f h_1 \cdot v_{qs} \tag{11}$$

$$\dot{y}_3 = L_f h_2 + L_{g2} h_2 \cdot v_{ds} \tag{12}$$

where $L_{g1} L_f h_1 = \frac{3}{2}\frac{p^2}{J}\frac{\lambda_m}{L_s}$

$$L_f h_2 = -\frac{R_s}{L_s} i_{ds} + \omega_r i_{qs}$$

$$L_{g2} h_2 = \frac{1}{L_s}$$

$$L_f^2 h_1 = \frac{3}{2}\frac{p^2}{J}\lambda_m\left(-\frac{R_s}{L_s} i_{qs} - \omega_r i_{ds} - \frac{\lambda_m}{L_s}\omega_r\right) - \frac{B}{J}\left(\frac{3}{2}\frac{p^2}{J}\lambda_m i_{qs} - \frac{B}{J}\omega_r - \frac{p}{J}T_L\right).$$

To linearize and decouple (10)-(12), the control input voltages v_{qs}^* and v_{ds}^* can be expressed as follows:

$$\begin{pmatrix} v_{qs}^* \\ v_{ds}^* \end{pmatrix} = D(x)^{-1}\begin{pmatrix} -L_f^2 h_1 + u_1 \\ -L_f h_2 + u_2 \end{pmatrix} \tag{13}$$

where u_1 and u_2 are the new control inputs by which the desired output error dynamics can be assigned, and $D(x)$ is the decoupling matrix defined as

$$D(x) = \begin{pmatrix} L_{g1} L_f h_1 & 0 \\ 0 & L_{g2} h_2 \end{pmatrix}. \tag{14}$$

Using (13), (10)-(12) become a linear decoupled model of Brunovski canonical form as

$$\dot{y}_1 = y_2 \tag{15}$$

$$\dot{y}_2 = u_1 \tag{16}$$

$$\dot{y}_3 = u_2 . \tag{17}$$

To assign the output error dynamics having the desired dynamic behavior, the new control inputs are designed by using a linear state feedback control law as follows:

$$u_1 = -k_{\omega 1}(y_1 - \omega_r^*) - k_{\omega 2}(y_2 - \dot{\omega}_r^*) + \ddot{\omega}_r^* \tag{18}$$

$$u_2 = -k_{id}(y_3 - i_{ds}^*) + \dot{i}_{ds}^* \tag{19}$$

where ω_r^* and i_{ds}^* are the commands for the speed and d-axis current, respectively. Then, this linear state feedback

control gives the second order speed error dynamics and the first order d-axis current error dynamics as follows:

$$(s^2 + k_{\omega 2}s + k_{\omega 1})e_\omega = se_\omega(0) + \dot{e}_\omega(0) \quad (20)$$

$$(s + k_{id})e_{id} = e_{id}(0) \quad (21)$$

where $e_\omega = \omega_r - \omega_r^*$, $e_{id} = i_{ds} - i_{ds}^*$, and s is a Laplace operator. The desired poles can be easily chosen by adjusting the controller gains $k_{\omega 1}$, $k_{\omega 2}$, and k_{id}.

This control scheme has some limitations. In order to implement the linear control law, the new state variables y must be available. It is, however, difficult to obtain the information on the acceleration since the acceleration signal cannot be easily measured and is very noisy. Thus, it has to be obtained from the original measured states x and motor parameters using (8). If there are some parameter variations or uncertainties on the model, these will cause errors in the transformation into the new state y as well as in the computation of the control input voltages in (13), which results in the output speed error.

IV. CONTROLLER DESIGN USING ADAPTIVE INPUT-OUTPUT LINEARIZATION TECHNIQUE

A. Modeling considering unknown disturbance torque and flux linkage variation

From the relationship between the developed torque and the mechanical load, the torque equation of the machine can be expressed using the nominal parameters as follows:

$$T_e = J_o\left(\frac{1}{p}\right)\frac{d\omega_r}{dt} + B_o\left(\frac{1}{p}\right)\omega_r + T_d \quad (22)$$

$$T_d = \Delta J\left(\frac{1}{p}\right)\frac{d\omega_r}{dt} + \Delta B\left(\frac{1}{p}\right)\omega_r + T_L \quad (23)$$

where $\Delta J = J - J_o$, $\Delta B = B - B_o$, subscript "$_o$" denotes the nominal value, and T_d is the effective load disturbance. Using (22), the speed dynamics is expressed as

$$\dot{\omega}_r = \frac{3}{2}\frac{p^2}{J_o}\lambda_m i_{qs} - \frac{B_o}{J_o}\omega_r - \frac{p}{J_o}T_d. \quad (24)$$

Under the assumption that the disturbance torque and flux linkage are unknown parameters, (4) can be rewritten using the estimated values as follows:

$$\dot{x} = \hat{f}(x) + g_1 v_{qs} + g_2 v_{ds} + d_1\Delta T_d + d_2\Delta\lambda_m \quad (25)$$

where $\Delta T_d = T_d - \hat{T}_d$, $\Delta\lambda_m = \lambda_m - \hat{\lambda}_m$

$$d_1 = \begin{pmatrix} -\frac{p}{J_o} & 0 & 0 \end{pmatrix}^T,\quad d_2 = \begin{pmatrix} \frac{3}{2}\frac{p^2}{J_o}i_{qs} & -\frac{\omega_r}{L_s} & 0 \end{pmatrix}^T$$

$$\hat{f}(x) = \begin{pmatrix} \frac{3}{2}\frac{p^2}{J_o}\hat{\lambda}_m i_{qs} - \frac{B_o}{J_o}\omega_r - \frac{p}{J_o}\hat{T}_d \\ -\frac{R_s}{L_s}i_{qs} - \omega_r i_{ds} - \frac{\hat{\lambda}_m}{L_s}\omega_r \\ -\frac{R_s}{L_s}i_{ds} + \omega_r i_{qs} \end{pmatrix}$$

and "^" denotes the estimated value.

B. Adaptive input-output linearization technique

To linearize the nonlinear state equation in (25), the new state variables are defined as follows:

$$z_1 = h_1(x) = \omega_r \quad (26)$$

$$z_2 = L_{\hat{f}}h_1(x) = \frac{3}{2}\frac{p^2}{J_o}\hat{\lambda}_m i_{qs} - \frac{B_o}{J_o}\omega_r - \frac{p}{J_o}\hat{T}_d \quad (27)$$

$$z_3 = h_2(x) = i_{ds} \quad (28)$$

where z_1 is the speed, z_2 is the computed acceleration using the estimated parameter values, and z_3 is the d-axis current. The state z_2 is employed for the implementation of the linear control law instead of the real acceleration. As $\hat{\lambda}_m$ and $\hat{T}_d$ converge to their real values, z_2 converges to the real acceleration signal. By using (26)-(28) as the state variables, (25) can be rewritten as follows:

$$\dot{z}_1 = z_2 + L_{d1}h_1 \cdot \Delta T_d + L_{d2}h_1 \cdot \Delta\lambda_m \quad (29)$$

$$\dot{z}_2 = L_{\hat{f}}^2 h_1 + L_{g1}L_{\hat{f}}h_1 \cdot v_{qs} + \frac{d}{dt}\hat{T}_d \cdot L_{d1}h_1 + \frac{d}{dt}\hat{\lambda}_m \cdot L_{d2}h_1 + L_{d1}L_{\hat{f}}h_1 \cdot \Delta T_d + L_{d2}L_{\hat{f}}h_1 \cdot \Delta\lambda_m \quad (30)$$

$$\dot{z}_3 = L_{\hat{f}}h_2 + L_{g2}h_2 \cdot v_{ds} \quad (31)$$

where $L_{d1}h_1 = -\frac{p}{J_o}$, $L_{d2}h_1 = \frac{3}{2}\frac{p^2}{J_o}i_{qs}$

$$L_{g1}L_{\hat{f}}h_1 = \frac{3}{2}\frac{p^2}{J_o}\frac{\hat{\lambda}_m}{L_s},\quad L_{d1}L_{\hat{f}}h_1 = \frac{pB_o}{J_o^2}$$

$$L_{d2}L_{\hat{f}}h_1 = -\frac{3}{2}\frac{p^2}{J_o}\left(\frac{\hat{\lambda}_m}{L_s}\omega_r + \frac{B_o}{J_o}i_{qs}\right)$$

$$L_{\hat{f}}h_2 = -\frac{R_s}{L_s}i_{ds} + \omega_r i_{qs}$$

$$L_{\hat{f}}^2 h_1 = \frac{3}{2}\frac{p^2}{J_o}\hat{\lambda}_m\left(-\frac{R_s}{L_s}i_{qs} - \omega_r i_{ds} - \frac{\hat{\lambda}_m}{L_s}\omega_r\right) - \frac{B_o}{J_o}\left(\frac{3}{2}\frac{p^2}{J_o}\hat{\lambda}_m i_{qs} - \frac{B_o}{J_o}\omega_r - \frac{p}{J_o}\hat{T}_d\right).$$

To linearize the nonlinear equations in (29)-(31), the control input voltages can be expressed as follows:

$$\begin{pmatrix} v_{qs}^* \\ v_{ds}^* \end{pmatrix} = D_a(x)^{-1}\begin{pmatrix} -L_{\hat{f}}^2 h_1 - \frac{d}{dt}\hat{T}_d \cdot L_{d1}h_1 - \frac{d}{dt}\hat{\lambda}_m \cdot L_{d2}h_1 + u_{a1} \\ -L_{\hat{f}}h_2 + u_{a2} \end{pmatrix} \quad (32)$$

where u_{a1} and u_{a2} are the linear control inputs which assign the output error dynamics, and the decoupling matrix $D_a(x)$ is defined as

$$D_a(x) = \begin{pmatrix} L_{g1}L_{\hat{f}}h_1 & 0 \\ 0 & L_{g2}h_2 \end{pmatrix}. \quad (33)$$

Note that the estimated value $\hat{\lambda}_m$ is used in $D_a(x)$ for the calculation of $L_{g1}L_{\hat{f}}h_1$. In contrast to $D(x)$, $D_a(x)$ becomes singular if the estimated flux linkage reaches a particular value. This value can be obtained using $\det D_a(x) = 0$ as $\hat{\lambda}_m = 0$. This singularity has to be considered in the adaptation process. Everywhere except for this singular point, the control input voltages in (32) can be always obtained. Using (32), the nonlinear motor

model becomes an incompletely linearized model and can be expressed as

$$\dot{z}_1 = z_2 + L_{d1}h_1 \cdot \Delta T_d + L_{d2}h_1 \cdot \Delta\lambda_m \quad (34)$$

$$\dot{z}_2 = u_{a1} + L_{d1}L_{\hat{f}}h_1 \cdot \Delta T_d + L_{d2}L_{\hat{f}}h_1 \cdot \Delta\lambda_m \quad (35)$$

$$\dot{z}_3 = u_{a2} \ . \quad (36)$$

Fig. 1 shows the block diagram of the resultant output dynamics after the linearization. As a result of the incomplete linearization, the nonlinear disturbances exist in its input-output relation. Such disturbances yield a steady-state error and a large transient in the speed response. Using the transformed state z, the linear control law is selected as follows:

$$u_{a1} = -k_{\omega 1}(z_1 - \omega_r^*) - k_{\omega 2}(z_2 - \dot{\omega}_r^*) + \ddot{\omega}_r^* \quad (37)$$

$$u_{a2} = -k_{id}(z_3 - i_{ds}^*) + \dot{i}_{ds}^* \ . \quad (38)$$

C. Estimations of disturbance torque and flux linkage

The disturbance torque and flux linkage will be simultaneously estimated using an MRAS technique. Using the linear decoupled model in (15)-(17) and the linear control law in (18) and (19), a reference model can be chosen as

$$\dot{z}_M = A_M z_M + U \quad (39)$$

where $z_M = [z_{1M} \quad z_{2M} \quad z_{3M}]^T$

$$A_M = \begin{pmatrix} 0 & 1 & 0 \\ -k_{\omega 1} & -k_{\omega 2} & 0 \\ 0 & 0 & -k_{id} \end{pmatrix}, \ U = \begin{pmatrix} 0 \\ k_{\omega 1}\omega_r^* + k_{\omega 2}\dot{\omega}_r^* + \ddot{\omega}_r^* \\ k_{id}i_{ds}^* + \dot{i}_{ds}^* \end{pmatrix} .$$

This reference model represents a desired output dynamic behavior, which is resulted from imposing a linear control law on the linearized model under the assumption of the parameter matching. An adjustable model can be obtained from the incompletely linearized model in (34)-(36) and the corresponding linear control law in (37) and (38) as follows:

$$\dot{z} = A_M z + U + B_1 \cdot \Delta T_d + B_2 \cdot \Delta\lambda_m \quad (40)$$

where $B_1 = (L_{d1}h_1 \quad L_{d1}L_{\hat{f}}h_1 \quad 0)^T$

$$B_2 = (L_{d2}h_1 \quad L_{d2}L_{\hat{f}}h_1 \quad 0)^T .$$

By subtracting the reference model from the adjustable model, the error dynamic equation can be obtained as follows:

$$\dot{\tilde{z}} = A_M \tilde{z} - W \quad (41)$$

where $\tilde{z} = z - z_M$ and $W = -B_1 \cdot \Delta T_d - B_2 \cdot \Delta\lambda_m$. From this error dynamic equation, the adaptation mechanism can be defined as

$$v = P\tilde{z} \quad (42)$$

$$\hat{T}_d(v,t) = \int_0^t \Psi_1(v,t)d\tau + \Psi_2(v,t) + \hat{T}_d(0) \quad (43)$$

$$\hat{\lambda}_m(v,t) = \int_0^t \Phi_1(v,t)d\tau + \Phi_2(v,t) + \hat{\lambda}_m(0) \quad (44)$$

where P is a symmetric positive definite matrix, Ψ_1, Ψ_2, Φ_1, and Φ_2 are the nonlinear adaptation mechanisms for the estimations of the disturbance torque and flux linkage, and $\hat{T}_d(0)$ and $\hat{\lambda}_m(0)$ are the initial estimates. The design procedures to obtain the asymptotic adaptation become as follows:

1. Determine P, Ψ_1, Ψ_2, Φ_1, and Φ_2 such that $\lim_{t\to\infty} \tilde{z}(t) = 0$ for any initial conditions $z_M(0)$ and $z(0)$
2. Find the supplementary conditions which lead to $\lim_{t\to\infty} \hat{T}_d(v,t) = T_d$ and $\lim_{t\to\infty} \hat{\lambda}_m(v,t) = \lambda_m$.

Based on (41)-(44), an MRAS structure can be constructed as shown in Fig. 2, which consists of a linear time invariant forward block and a nonlinear feedback block. This system is hyperstable if the forward transfer function matrix is strictly positive real and the input-output inner product of the nonlinear feedback block satisfies the Popov's integral inequality as follows [12]:

$$\int_0^{t_1} v^T W dt = \int_0^{t_1} (-v^T B_1 \cdot \Delta T_d - v^T B_2 \cdot \Delta\lambda_m)dt \geq -\gamma_o^2 \quad \text{for all } t_1 \geq 0 \quad (45)$$

where γ_o^2 is a finite positive constant. It is shown that for a given matrix A_M, the strictly positive real transfer function matrix

$$H(s) = P(sI - A_M)^{-1} \quad (46)$$

can be obtained by choosing P as the solution of the Lyapunov equation as follows:

$$A_M^T P + PA_M = -Q \quad (47)$$

where Q is a symmetric positive definite matrix. If and only if the reference model is asymptotically stable, which is generally the case, (47) always has a positive definite matrix solution P. In order to derive the adaptation mechanisms, (45) can be expressed using (43) and (44) as follows:

$$\int_0^{t_1} -v^T B_1 \cdot \left(T_d - \int_0^t \Psi_1(v,t)d\tau - \Psi_2(v,t) - \hat{T}_d(0) \right) dt + \int_0^{t_1} -v^T B_2 \cdot \left(\lambda_m - \int_0^t \Phi_1(v,t)d\tau - \Phi_2(v,t) - \hat{\lambda}_m(0) \right) dt \geq -\gamma_o^2 \quad (48)$$

To derive the adaptation mechanisms from (48), the estimated parameters need to be unknown constants or slowly-varying. Even though the disturbance torque T_d is not a constant parameter under the mechanical parameter variations such as the inertia and viscous friction coefficient, if the sampling interval is sufficiently fast as compared with the time variation of the unknown disturbance, the disturbance torque T_d can be assumed to be a constant during each sampling intervals as follows [10], [11]:

$$\dot{T}_d = 0 . \quad (49)$$

Using the above assumption, it is shown that the inequality in (48) can be satisfied by selecting the nonlinear adaptation mechanisms as follows [12]:

$$\Psi_1 = k_{IT}(v^T B_1) \quad (50)$$

$$\Psi_2 = k_{PT}(v^T B_1) \quad (51)$$

$$\Phi_1 = k_{I\lambda}(v^T B_2) \quad (52)$$

$$\Phi_2 = k_{P\lambda}(v^T B_2) \quad (53)$$

where k_{PT} and k_{IT} are the PI gains for the disturbance torque estimation, respectively, and $k_{P\lambda}$ and $k_{I\lambda}$ are the

PI gains for the flux linkage estimation, respectively. By substituting (50)-(53) into (43) and (44), the disturbance torque and flux linkage can be simultaneously estimated as follows:

$$\hat{T}_d(v,t)=\left(k_{PT}+\frac{k_{IT}}{s}\right)\cdot(v^T B_1)+\hat{T}_d(0) \tag{54}$$

$$\hat{\lambda}_m(v,t)=\left(k_{P\lambda}+\frac{k_{I\lambda}}{s}\right)\cdot(v^T B_2)+\hat{\lambda}_m(0) \tag{55}$$

with $v^T B_1 = v_1 \cdot L_{d1}h_1 + v_2 \cdot L_{d1}L_{\hat{f}}h_1$

$v^T B_2 = v_1 \cdot L_{d2}h_1 + v_2 \cdot L_{d2}L_{\hat{f}}h_1$

where $v=[v_1 \quad v_2 \quad v_3]^T$ and the nominal values T_{Lo} and λ_{mo} are used for the initial estimates of $\hat{T}_d(0)$ and $\hat{\lambda}_m(0)$, respectively.

V. SIMULATION AND EXPERIMENTS

A. Configuration of overall system

The overall block diagram for the proposed control scheme is shown in Fig. 3. The overall system consists of a reference model, an adjustable model, and an adaptation mechanism. In this figure, the large shaded area represents the adjustable model resulting from the parameter mismatch between the speed controller and motor. During the operations, the transformed state z is continuously compared with the model output z_M. The difference $\tilde{z}$ is used in the adaptation mechanism to update the controller parameters used in the adjustable model. The computed reference voltage vector v_s^* are applied to a BLDC motor using the space vector PWM technique [13].

The configuration of the experimental system is shown in Fig. 4. The whole speed control algorithms including the space vector PWM technique are implemented by the assembly language program using DSP TMS320C30 with a clock frequency of 32 MHz. The sampling period is set to 128 [μsec]. The BLDC motor is driven by a three-phase PWM inverter employing the intelligent power module (IPM) with a switching frequency of 7.8 kHz. The rotor speed and absolute rotor position are detected through a 12 bit/rev resolver-to-digital converter (RDC) using a brushless resolver. The nominal parameters of a BLDC motor are listed in Table I.

Table. I Specifications of a BLDC motor

Rated power	400 W	Rated speed	3000 rpm
Rated torque	1.274 Nm	Number of poles	4
Magnetic flux	0.17 Wb	Stator resistance	3.0 ohm
Stator inductance	10.5 mH	Moment of inertia	1.54×10^{-4} $Nm\cdot s^2$

B. Experimental results

The d-axis current command is given as zero and the speed trajectory command is given as follows:

$$\omega_r^* = \frac{\omega_{rf}}{T}t - \frac{\omega_{rf}}{2\pi}\sin\left(\frac{2\pi t}{T}\right) \tag{56}$$

$$\dot{\omega}_r^* = \frac{\omega_{rf}}{T} - \frac{\omega_{rf}}{T}\cos\left(\frac{2\pi t}{T}\right) \tag{57}$$

$$\ddot{\omega}_r^* = 2\pi\frac{\omega_{rf}}{T^2}\sin\left(\frac{2\pi t}{T}\right) \tag{58}$$

where ω_{rf} is the desired final speed and T is the time when the speed command reaches from zero to ω_{rf}. Fig. 5 shows the Experimental results for the linear control law in (37) and (38) under the nominal parameters without adaptation algorithms. The gains of the linear control law are selected as $k_{\omega 2}=140$, $k_{\omega 1}=9800$, and $k_{id}=1000$ so that the poles of the speed error dynamics and the d-axis current error dynamics are determined as $-70\pm j70$ and -1000, respectively. Under the nominal parameter values, the speed command can be well tracked. Also, the computed acceleration z_2 is effectively controlled to the acceleration command. Fig. 6 shows the experimental results of the proposed control scheme when $\Delta\lambda_m$ is initially -20 % of its nominal value. It is shown that the speed response is unaffected by this variation and gives the desired dynamic performance and zero steady-state error. The computed acceleration z_2 using the estimated parameters shows a large transient error because of the flux linkage variation. However, as the flux linkage and disturbance torque are estimated, z_2 is well controlled to the acceleration command. The experimental results for the inertia variation are shown in Figs. 7-9. Without the adaptation algorithms, the speed response shows the undesirable dynamic performance under the inertia variation as shown in Fig. 7. Under both the flux linkage and inertia variations, the speed response shows the undesirable dynamic performance as well as the steady-state error as shown in Fig. 8. In the proposed scheme, however, the speed response shows a good dynamic performance as a result of an effective simultaneous parameter estimations as shown in Fig. 9. The gains of the linear control law are set as the same as the non-adaptive case. The PI gains for the adaptation algorithms are chosen as follows: $k_{PT}=1\times10^{-4}$, $k_{IT}=5\times10^{-3}$, $k_{P\lambda}=0$, $k_{I\lambda}=3\times10^{-6}$, and $Q=diag(1 \quad 5\times10^{-3} \quad 1)$.

VI. CONCLUSIONS

A robust speed control method of a BLDC motor using an adaptive input-output linearization technique has been proposed. By using this method, a systematic design approach for a speed controller can be accomplished without considering a separate inner-loop current regulator. Under the parameter variations, the input-output linearization scheme with the linear control law yields the steady-state errors as well as the deteriorated transient responses as a result of the incomplete linearization. To overcome this limitation, the system parameters are estimated using an MRAS technique where the disturbance torque and the magnitude of the flux linkage can be simultaneously estimated. The estimated parameters are

used for the input-output linearization to obtain a robust control performance. Thus, a speed control performance is not affected by the load torque disturbance and the variation of the motor and mechanical parameters. Through the comparative experimental results, it is verified that the proposed control scheme yields a robust output performance even under the presence of the variation of the motor parameter and the external disturbances caused by the inertia variation and step load change.

REFERENCES

[1] P. C. Krause, *Analysis of Electric Machinery*, McGraw-Hill, New York, 1986.

[2] D. M. Brod, and D. W. Novotny, "Current control of VSI-PWM inverters," *IEEE Trans. Industry Applications*, vol. 21, no. 2, pp. 562-570, March/April 1985.

[3] J. J. Carroll Jr., and D. M. Dawson, "Integrator backstepping techniques for the tracking control of permanent magnet brush dc motors," *IEEE Trans. Industry Applications*, vol. 31, no. 2, pp. 248-255, March/April 1995.

[4] J. J. E. Slotine, and W. Li, *Applied Nonlinear Control*, Prentice-Hall International Editions, 1991.

[5] P. D. Olivier, "Feedback linearization of dc motors," *IEEE Trans. Industrial Electronics*, vol. 38, no. 6, pp. 498-501, Nov. 1991.

[6] A. Bellini, G. Figalli, and F. Tosti, "Linearized model of induction motor drives via nonlinear state feedback decoupling," in Proceedings of the 1991 EPE, Firenze.

[7] T. von Raumer, J. M. Dion, L. Dugard, and J. L. Thomas, "Applied nonlinear control of an induction motor using digital signal processing," *IEEE Trans. Control System Technology*, vol. 2, no. 4, pp. 327-335, Dec. 1994.

[8] L. A. Pereira, and E. M. Hemerly, "Design of an adaptive linearizing control for induction motors," IEEE IECON '95 conference record, pp. 1012-1016, 1995.

[9] B. Le Pioufle, "Comparison of speed nonlinear control strategies for the synchronous servomotor," *Electric Machines and Power Systems*, vol. 21, pp. 151-169, 1993.

[10] N. Matsui, T. Makino, and H. Satoh, "Autocompensation of torque ripple of direct drive motor by torque observer," *IEEE Trans. Industry Applications*, vol. 29, no. 1, pp. 187-194, Jan./Feb. 1993.

[11] J. S. Ko, J. H. Lee, and M. J. Youn, "Robust digital position control of brushless DC motor with adaptive load torque observer," *IEE Proc. Electr. Power Appl.* vol. 141, no. 2, pp. 63-70, 1994.

[12] Y. D. Landau, *Adaptive Control-The Model Reference Approach*, Marcel Dekker, New York, 1979.

[13] H. W. van der Broeck, H. C. Skudelny, and G. V. Stanke, "Analysis and realization of a pulsewidth modulator based on voltage space vectors," *IEEE Trans. Industry Applications*, vol. IA-24, no. 1, pp. 142-150, Jan./Feb. 1988.

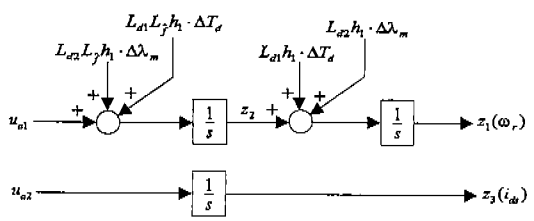

Fig. 1 Block diagram of the incompletely linearized output dynamics

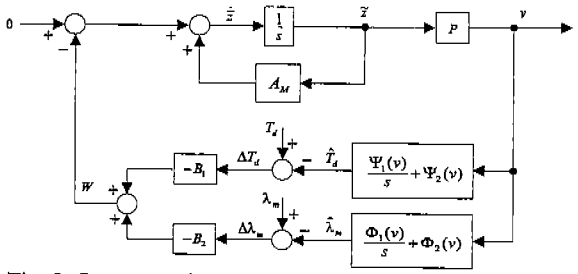

Fig. 2 Structure of MRAS for the estimations of the disturbance torque and flux linkage

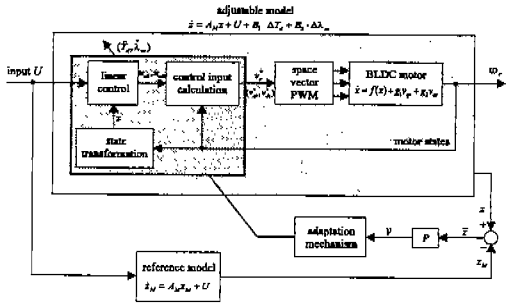

Fig. 3 Overall block diagram for the proposed scheme

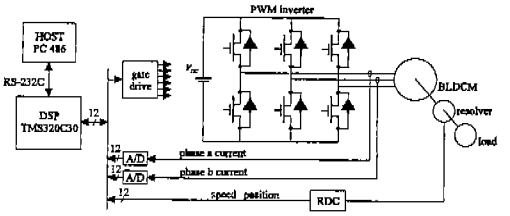

Fig. 4 Configuration of experimental system

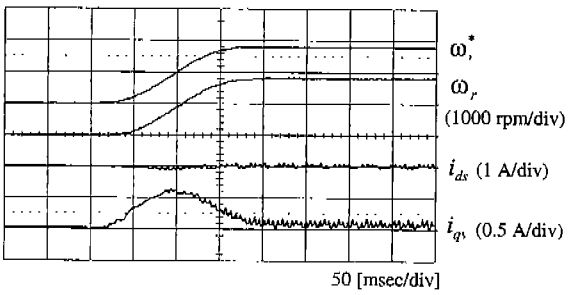

(a) speed transient response

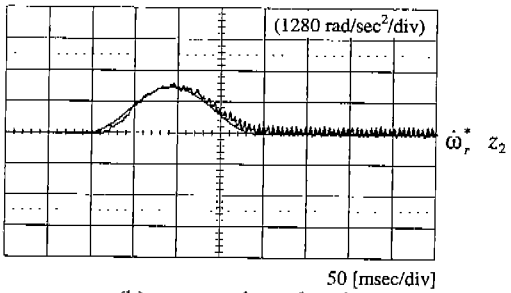

(b) computed acceleration

Fig. 5 Experimental results for the linear control law under the nominal parameters without adaptation algorithms

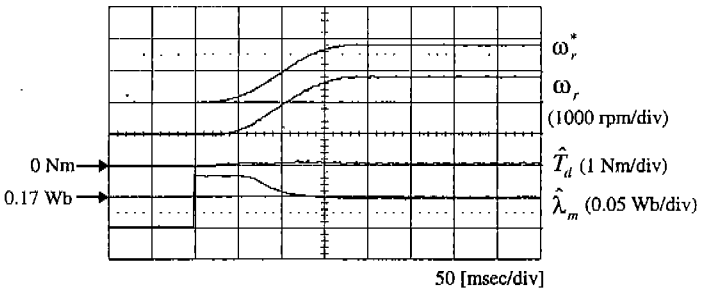

(a) speed transient response

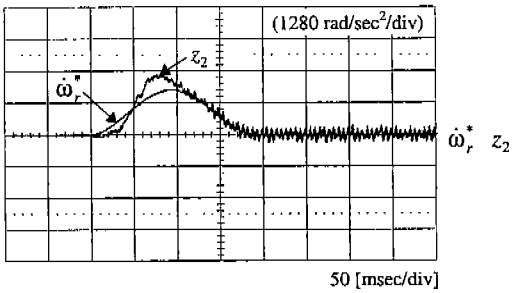

(b) computed acceleration using estimated parameters

Fig. 6 Experimental results of the proposed control scheme under the flux linkage variation

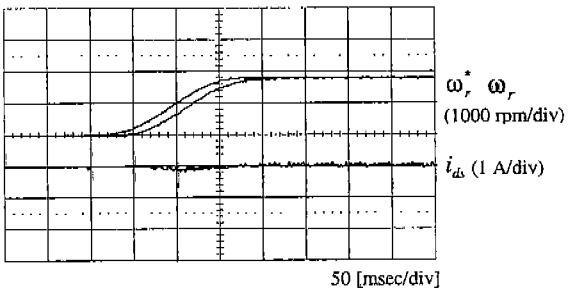

Fig. 7 Experimental results of the linear control law under the inertia variation without adaptation algorithms

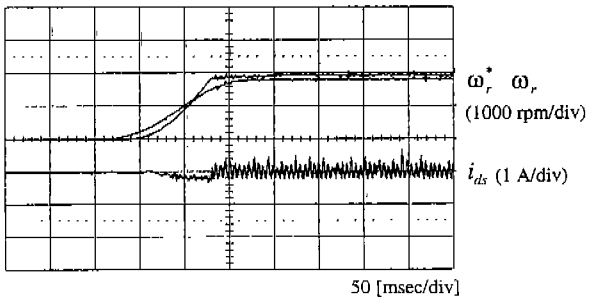

Fig. 8 Experimental result of the linear control law under both the flux linkage and inertia variations without adaptation algorithms

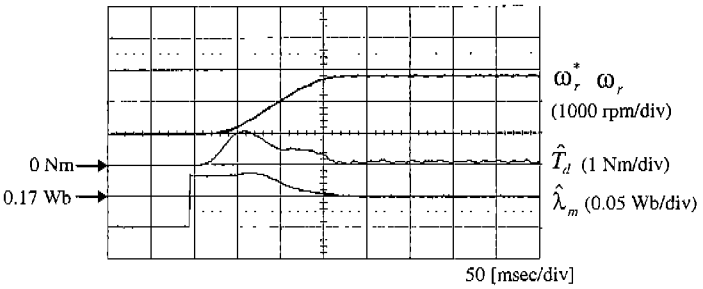

Fig. 9 Experimental results of the proposed control scheme under both the flux linkage and inertia variations